Mathematics

https://www.aimspress.com/journal/Math

AIMS Mathematics, 10(3): 5568–5582.
DOI: 10.3934/math.2025257
Received: 19 January 2025
Revised: 02 March 2025
Accepted: 05 March 2025
Published: 12 March 2025

Research article

An efficient and energy-stable scheme for the modified phase-field crystal equation with a strong nonlinear vacancy potential

Hyun Geun Lee*

Department of Mathematics, Dongguk University, Seoul 04620, Republic of Korea

* **Correspondence:** Email: leeh1@dongguk.edu.

Abstract: In this paper, we present an efficient and energy-stable scheme based on the Crank–Nicolson formula for the modified phase-field crystal equation with a strong nonlinear vacancy potential. In the scheme, the nonlinear terms (the first derivatives of the double-well and vacancy potentials) are treated explicitly, which makes the scheme efficient, and the energy stability is guaranteed by assuming that the second derivatives of the double-well and vacancy potentials are each bounded and by adding two second-order stabilization terms. In particular, by bounding the second derivatives of the double-well and vacancy potentials, respectively, we can choose the stabilization parameters independently of the vacancy parameter. As a result, the convergence constant and energy decay trend are not affected by the vacancy parameter.

Keywords: modified phase-field crystal equation; strong nonlinear vacancy potential; efficiency; energy stability
Mathematics Subject Classification: 65M06, 65N06

1. Introduction

Phase-field models have emerged as a powerful computational approach to modeling and predicting mesoscale morphological and microstructure evolution in materials [1], such as crystals [2, 3], data assimilation [4], and nucleation [5]. As one example, the modified phase-field crystal (MPFC) equation was adopted to describe diffusive dynamics and elastic interactions [6–11] and extended to the MPFC equation with a strong nonlinear vacancy potential (VMPFC) to include vacancies that exist in real materials when the local density is low [12]. We consider the following energy functional [12]:

$$\mathcal{E}(\phi) := \int_\Omega \left(F_{dou}(\phi) + F_{vac}(\phi) + \frac{1}{2}\phi(1+\Delta)^2\phi \right) d\mathbf{x}, \tag{1.1}$$

where Ω is a domain in $\mathbb{R}^d$ $(d = 2, 3)$, ϕ is the local atomic density field, $F_{dou}(\phi) = \frac{1}{4}\phi^4 - \frac{\epsilon}{2}\phi^2$ is the

double-well potential, $\epsilon > 0$ is the undercooling parameter, $F_{vac}(\phi) = \frac{h_{vac}}{3}(|\phi|^3 - \phi^3)$ is the vacancy potential, and $h_{vac} \gg 1$ is the penalization parameter. For simplicity, we take the periodic boundary condition for the system. Then, the VMPFC equation can be regarded as a pseudo-gradient flow of (1.1) in $H^{-1}(\Omega)$:

$$\alpha\frac{\partial\psi}{\partial t} + \beta\psi = M\Delta\left(f_{dou}(\phi) + f_{vac}(\phi) + (1+\Delta)^2\phi\right), \tag{1.2}$$

$$\frac{\partial\phi}{\partial t} = \psi, \tag{1.3}$$

where $\alpha, \beta > 0$ are constants, $M > 0$ is a mobility, $f_{dou}(\phi) = F'_{dou}(\phi)$, and $f_{vac}(\phi) = F'_{vac}(\phi)$. When $\alpha = h_{vac} = 0$, the VMPFC equation degenerates back to the classical PFC equation. The initial condition of the VMPFC equation is

$$\psi(\mathbf{x}, 0) = \psi^0(\mathbf{x}), \quad \phi(\mathbf{x}, 0) = \phi^0(\mathbf{x}).$$

The VMPFC equation becomes a mass-conservative equation if $\left(\psi^0(\mathbf{x}), \mathbf{1}\right)_{L^2} = 0$ is used and the solution of the VMPFC equation decays the following energy functional:

$$\mathcal{F}(\phi) := \mathcal{E}(\phi) + \frac{\alpha}{2M}\|\psi\|^2_{H^{-1}}, \tag{1.4}$$

where $(\cdot,\cdot)_{L^2}$ and $(\cdot,\cdot)_{H^{-1}}$ denote the inner products in $L^2(\Omega)$ and $H^{-1}(\Omega)$, respectively. The H^{-1} inner product is defined as follows: for given $f, g \in H_0$ (H_0 is a zero average subspace of a Hilbert space), $(f,g)_{H^{-1}} := (\nabla v_f, \nabla v_g)_{L^2}$, where $v_f, v_g \in H_0$ are the solutions of the periodic boundary value problems $-\Delta v_f = f$, $-\Delta v_g = g$ in Ω, respectively. And $\|\cdot\|_{H^{-1}} := \sqrt{(\cdot,\cdot)_{H^{-1}}}$ denotes the H^{-1} norm.

Various numerical schemes have been proposed to solve the VMPFC equation [13–18]. The scalar auxiliary variable, $u(t) = \sqrt{\int_\Omega (F_{dou}(\phi) + F_{vac}(\phi))\, d\mathbf{x} + C_u}$, the multiple scalar auxiliary variables, $u_1(t) = \sqrt{\int_\Omega F_{dou}(\phi)\, d\mathbf{x} + C_{u_1}}$ and $u_2(t) = \sqrt{\int_\Omega F_{vac}(\phi)\, d\mathbf{x} + C_{u_2}}$, the auxiliary variable, $v(\mathbf{x}, t) = \sqrt{F_{dou}(\phi) + F_{vac}(\phi) + C_v}$, and the exponential scalar auxiliary variable, $w(t) = \exp\left(\frac{\mathcal{F}(\phi)}{C_w}\right)$, were introduced in [13], [14, 15], [16], and [17], respectively, to redefine the energy functional and reformulate the VMPFC equation, where C_u, C_{u_1}, C_{u_2}, and C_v are constants that make each radicand positive and C_w is a constant that suppresses the exponential growth. And the second-order backward differentiation formula was used to discretize the reformulated system, and the second-order stabilization term, $S(\phi^{n+1} - 2\phi^n + \phi^{n-1})$, was added to improve energy stability. In [18], the linear convex splitting was introduced by truncating $\frac{1}{4}\phi^4 + F_{vac}(\phi)$ by the specific function and the second-order Douglas–Dupont regularization, $-S\,\Delta t\Delta(\phi^{n+1} - \phi^n)$, was added to improve energy stability. For the balance between accuracy and energy stability, S was chosen to be $h_{vac}O(|\min_{\mathbf{x}\in\Omega}(\phi(\mathbf{x}, t), 0)|)$ in [13] and proportional to h_{vac} in [14–18]. Thus, it was observed that the convergence constant and energy decay trend are affected by h_{vac}.

In this paper, we present an efficient and energy-stable scheme based on the Crank–Nicolson (CN) formula for the VMPFC equation. In the scheme, $f_{dou}(\phi)$ and $f_{vac}(\phi)$ are treated explicitly, which makes the scheme efficient, and the energy stability is guaranteed by assuming that $f'_{dou}(\phi)$ and $f'_{vac}(\phi)$ are each bounded and by adding two second-order stabilization terms. In particular, by bounding $f'_{dou}(\phi)$ and $f'_{vac}(\phi)$ respectively, we can choose the stabilization parameters independently of h_{vac}. As a result, the

convergence constant and energy decay trend are not affected by h_{vac}. And the scheme can be easily implemented within a few lines of MATLAB code.

The remainder of this paper is organized as follows. We design the numerical approximation and show its mass conservation and energy stability analytically in Section 2 and numerically in Section 3. Conclusions are given in Section 4. The MATLAB code for the numerical approximation is given in the Appendix.

2. Efficient and energy-stable scheme

We design the numerical approximation for the VMPFC equation based on the CN formula:

$$\begin{aligned}\frac{\alpha}{\Delta t}\delta_t\psi^{n+1} &= M\Delta\left(f_{dou}(\phi^{*,n+\frac{1}{2}}) + f_{vac}(\phi^{*,n+\frac{1}{2}}) + (1+\Delta)^2\phi^{n+\frac{1}{2}} - A\Delta t\Delta\delta_t\phi^{n+1} + B(\delta_t\phi^{n+1} - \delta_t\phi^n)\right)\\ &\quad -\beta\psi^{n+\frac{1}{2}}, \qquad (2.1)\\ \frac{1}{\Delta t}\delta_t\phi^{n+1} &= \psi^{n+\frac{1}{2}}, \qquad (2.2)\end{aligned}$$

where $\delta_t\phi^{n+1} = \phi^{n+1} - \phi^n$, $\phi^{n+\frac{1}{2}} = \frac{\phi^{n+1}+\phi^n}{2}$, $\phi^{*,n+\frac{1}{2}} = \frac{3\phi^n - \phi^{n-1}}{2}$, $\delta_t\psi^{n+1} = \psi^{n+1} - \psi^n$, $\psi^{n+\frac{1}{2}} = \frac{\psi^{n+1}+\psi^n}{2}$, $A, B > 0$ are stabilization parameters, and $\phi^{-1} \equiv \phi^0$.

Theorem 1. *The scheme* (2.1)-(2.2) *with* $\left(\psi^0, \mathbf{1}\right)_{L^2} = 0$ *is mass conserving.*

Proof. Suppose that the scheme (2.1)-(2.2) has a solution. From Eq (2.1), we have

$$\frac{\alpha}{\Delta t}\left(\delta_t\psi^{n+1}, \mathbf{1}\right)_{L^2} = -\beta\left(\psi^{n+\frac{1}{2}}, \mathbf{1}\right)_{L^2},$$

by the periodic boundary condition. This gives the relation

$$\left(\frac{2\alpha}{\Delta t} + \beta\right)\left(\psi^{n+\frac{1}{2}}, \mathbf{1}\right)_{L^2} = \frac{2\alpha}{\Delta t}\left(\psi^n, \mathbf{1}\right)_{L^2}.$$

With $\left(\psi^0, \mathbf{1}\right)_{L^2} = 0$, the relation ensures that

$$\left(\psi^{n+\frac{1}{2}}, \mathbf{1}\right)_{L^2} = 0, \quad \text{i.e.,} \quad \left(\delta_t\phi^{n+1}, \mathbf{1}\right)_{L^2} = \left(\phi^{n+1} - \phi^n, \mathbf{1}\right)_{L^2} = 0$$

for all $n \geq 0$. □

Before proving the unique solvability of the scheme (2.1)-(2.2), we simplify the scheme as follows:

$$\begin{aligned}\frac{\phi^{n+1} - \phi^n}{\Delta t} &= \frac{M\Delta t}{2\alpha + \beta\Delta t}\Delta\left(\frac{1}{2}(1+\Delta)^2\phi^{n+1} - A\Delta t\Delta\phi^{n+1} + B\phi^{n+1}\right) + \frac{M\Delta t}{2\alpha + \beta\Delta t}R + \frac{2\alpha}{2\alpha + \beta\Delta t}\psi^n, \qquad (2.3)\\ \psi^{n+1} &= 2\frac{\phi^{n+1} - \phi^n}{\Delta t} - \psi^n,\end{aligned}$$

where $R = \Delta\left(f_{dou}(\phi^{*,n+\frac{1}{2}}) + f_{vac}(\phi^{*,n+\frac{1}{2}}) + \frac{1}{2}(1+\Delta)^2\phi^n + A\Delta t\Delta\phi^n + B(-2\phi^n + \phi^{n-1})\right)$.

Theorem 2. *The scheme* (2.1)-(2.2) *with* $\left(\psi^0, \mathbf{1}\right)_{L^2} = 0$ *is uniquely solvable for any* $\Delta t > 0$.

Proof. We consider the following functional for ϕ defined in the constraint space $(\phi, \mathbf{1})_{L^2} = (\phi^n, \mathbf{1})_{L^2}$ given by Theorem 1:

$$\begin{aligned} G(\phi) &= \frac{1}{2\Delta t}\|\phi - \phi^n\|_{H^{-1}}^2 + \frac{M\Delta t}{2\alpha + \beta\Delta t}\left(\frac{1}{4}\|(1+\Delta)\phi\|_{L^2}^2 + \frac{A\Delta t}{2}\|\nabla\phi\|_{L^2}^2 + \frac{B}{2}\|\phi\|_{L^2}^2\right) \\ &\quad - \left(\frac{M\Delta t}{2\alpha + \beta\Delta t}R + \frac{2\alpha}{2\alpha + \beta\Delta t}\psi^n, \phi\right)_{H^{-1}}. \end{aligned}$$

It may be shown that ϕ^{n+1} is the unique minimizer of $G(\phi)$ if and only if it solves, for any φ with $(\varphi, \mathbf{1})_{L^2} = 0$,

$$\begin{aligned} \left.\frac{dG(\phi + \eta\varphi)}{d\eta}\right|_{\eta=0} &= \left(\frac{\phi - \phi^n}{\Delta t}, \varphi\right)_{H^{-1}} + \frac{M\Delta t}{2\alpha + \beta\Delta t}\left(\frac{1}{2}(1+\Delta)^2\phi - A\Delta t\Delta\phi + B\phi, \varphi\right)_{L^2} \\ &\quad - \left(\frac{M\Delta t}{2\alpha + \beta\Delta t}R + \frac{2\alpha}{2\alpha + \beta\Delta t}\psi^n, \varphi\right)_{H^{-1}} \\ &= \left(\frac{\phi - \phi^n}{\Delta t} - \frac{M\Delta t}{2\alpha + \beta\Delta t}\Delta\left(\frac{1}{2}(1+\Delta)^2\phi - A\Delta t\Delta\phi + B\phi\right), \varphi\right)_{H^{-1}} \\ &\quad - \left(\frac{M\Delta t}{2\alpha + \beta\Delta t}R + \frac{2\alpha}{2\alpha + \beta\Delta t}\psi^n, \varphi\right)_{H^{-1}} = 0, \end{aligned} \tag{2.4}$$

because $G(\phi)$ is strictly convex by

$$\left.\frac{d^2G(\phi + \eta\varphi)}{d\eta^2}\right|_{\eta=0} = \frac{1}{\Delta t}\|\varphi\|_{H^{-1}}^2 + \frac{M\Delta t}{2\alpha + \beta\Delta t}\left(\frac{1}{2}\|(1+\Delta)\varphi\|_{L^2}^2 + A\Delta t\|\nabla\varphi\|_{L^2}^2 + B\|\varphi\|_{L^2}^2\right) \geq 0.$$

And, Eq (2.4) is true for any φ if and only if the given equation holds:

$$\frac{\phi^{n+1} - \phi^n}{\Delta t} = \frac{M\Delta t}{2\alpha + \beta\Delta t}\Delta\left(\frac{1}{2}(1+\Delta)^2\phi^{n+1} - A\Delta t\Delta\phi^{n+1} + B\phi^{n+1}\right) + \frac{M\Delta t}{2\alpha + \beta\Delta t}R + \frac{2\alpha}{2\alpha + \beta\Delta t}\psi^n.$$

Hence, minimizing the strictly convex functional $G(\phi)$ is equivalent to solving Eq (2.3). □

To prove the energy stability of the scheme (2.1)-(2.2), we assume that there exist constants $L_1, L_2 > 0$ such that

$$\max_{\phi\in\mathbb{R}} |f'_{dou}(\phi)| \leq L_1 \quad \text{and} \quad \max_{\phi\in\mathbb{R}} |f'_{vac}(\phi)| \leq L_2. \tag{2.5}$$

Theorem 3. *Assume that* (2.5) *is satisfied. The scheme* (2.1)-(2.2) *with* $A \geq \frac{M(L_1+L_2)^2}{16\beta}$ *and* $B \geq \frac{L_1+L_2}{2}$ *fulfills the following energy inequality:*

$$\tilde{\mathcal{F}}^{n+1} \leq \tilde{\mathcal{F}}^n,$$

where

$$\tilde{\mathcal{F}}^{n+1} := \mathcal{F}(\phi^{n+1}) + \left(\frac{B}{2} + \frac{L_1 + L_2}{4}\right)\|\delta_t\phi^{n+1}\|_{L^2}^2. \tag{2.6}$$

Proof. By simple calculations,

$$\left(\delta_t\phi^{n+1}, (1+\Delta)^2\phi^{n+\frac{1}{2}}\right)_{L^2} = \frac{1}{2}\left(\|(1+\Delta)\phi^{n+1}\|_{L^2}^2 - \|(1+\Delta)\phi^n\|_{L^2}^2\right) \tag{2.7}$$

and

$$\begin{aligned}&\left(\delta_t\phi^{n+1}, -A\Delta t\Delta\delta_t\phi^{n+1} + B(\delta_t\phi^{n+1} - \delta_t\phi^n)\right)_{L^2}\\ &= A\Delta t\|\nabla\delta_t\phi^{n+1}\|_{L^2}^2 + \frac{B}{2}\left(\|\delta_t\phi^{n+1}\|_{L^2}^2 - \|\delta_t\phi^n\|_{L^2}^2 + \|\delta_t\phi^{n+1} - \delta_t\phi^n\|_{L^2}^2\right).\end{aligned} \tag{2.8}$$

And, for $i = dou$ and vac, to handle $f_i(\phi^{*,n+\frac{1}{2}})$, we expand $F_i(\phi^{n+1})$ and $F_i(\phi^n)$ at $\phi^{*,n+\frac{1}{2}}$ as

$$\begin{aligned}F_i(\phi^{n+1}) &= F_i(\phi^{*,n+\frac{1}{2}}) + f_i(\phi^{*,n+\frac{1}{2}})(\phi^{n+1} - \phi^{*,n+\frac{1}{2}}) + \frac{1}{2}f_i'(\xi^{n+1})(\phi^{n+1} - \phi^{*,n+\frac{1}{2}})^2,\\ F_i(\phi^n) &= F_i(\phi^{*,n+\frac{1}{2}}) + f_i(\phi^{*,n+\frac{1}{2}})(\phi^n - \phi^{*,n+\frac{1}{2}}) + \frac{1}{2}f_i'(\xi^n)(\phi^n - \phi^{*,n+\frac{1}{2}})^2,\end{aligned}$$

where ξ^{n+1} is a function that is pointwise bounded between ϕ^{n+1} and $\phi^{*,n+\frac{1}{2}}$ and ξ^n is a function that is pointwise bounded between ϕ^n and $\phi^{*,n+\frac{1}{2}}$. Then, we obtain

$$\begin{aligned}&\left(\delta_t\phi^{n+1}, f_i(\phi^{*,n+\frac{1}{2}})\right)_{L^2}\\ &= \left(F_i(\phi^{n+1}) - F_i(\phi^n), \mathbf{1}\right)_{L^2} - \frac{1}{2}\left(f_i'(\xi^{n+1}), (\phi^{n+1} - \phi^{*,n+\frac{1}{2}})^2\right)_{L^2} + \frac{1}{2}\left(f_i'(\xi^n), (\phi^n - \phi^{*,n+\frac{1}{2}})^2\right)_{L^2}\\ &= \left(F_i(\phi^{n+1}) - F_i(\phi^n), \mathbf{1}\right)_{L^2} - \frac{1}{2}\left(f_i'(\xi^{n+1}), \delta_t\phi^{n+1}(\delta_t\phi^{n+1} - \delta_t\phi^n)\right)_{L^2}\\ &\quad -\frac{1}{8}\left(f_i'(\xi^{n+1}) - f_i'(\xi^n), (\delta_t\phi^n)^2\right)_{L^2}.\end{aligned} \tag{2.9}$$

Using the identities (2.7)–(2.9),

$$\begin{aligned}&\mathcal{E}(\phi^{n+1}) + \frac{B}{2}\|\delta_t\phi^{n+1}\|_{L^2}^2 - \mathcal{E}(\phi^n) - \frac{B}{2}\|\delta_t\phi^n\|_{L^2}^2\\ &\le \frac{1}{M}\left(\delta_t\phi^{n+1}, \Delta^{-1}\left(\frac{\alpha}{\Delta t}\delta_t\psi^{n+1} + \beta\psi^{n+\frac{1}{2}}\right)\right)_{L^2} - A\Delta t\|\nabla\delta_t\phi^{n+1}\|_{L^2}^2 - \frac{B}{2}\|\delta_t\phi^{n+1} - \delta_t\phi^n\|_{L^2}^2\\ &\quad + \frac{L_1+L_2}{4}\left(\|\delta_t\phi^{n+1}\|_{L^2}^2 + \|\delta_t\phi^{n+1} - \delta_t\phi^n\|_{L^2}^2 + \|\delta_t\phi^n\|_{L^2}^2\right),\end{aligned}$$

where we have used the assumption (2.5). And

$$\frac{1}{M}\left(\delta_t\phi^{n+1}, \Delta^{-1}\left(\frac{\alpha}{\Delta t}\delta_t\psi^{n+1} + \beta\psi^{n+\frac{1}{2}}\right)\right)_{L^2} = -\frac{\alpha}{2M}\left(\|\psi^{n+1}\|_{H^{-1}}^2 - \|\psi^n\|_{H^{-1}}^2\right) - \frac{\beta}{M\Delta t}\|\delta_t\phi^{n+1}\|_{H^{-1}}^2.$$

By the definition of $\tilde{\mathcal{F}}$,

$$\begin{aligned}&\tilde{\mathcal{F}}^{n+1} - \tilde{\mathcal{F}}^n\\ &\le -\frac{\beta}{M\Delta t}\|\delta_t\phi^{n+1}\|_{H^{-1}}^2 - A\Delta t\|\nabla\delta_t\phi^{n+1}\|_{L^2}^2 + \frac{L_1+L_2}{2}\|\delta_t\phi^{n+1}\|_{L^2}^2 - \left(\frac{B}{2} - \frac{L_1+L_2}{4}\right)\|\delta_t\phi^{n+1} - \delta_t\phi^n\|_{L^2}^2\\ &\le -\left(\frac{\beta}{M\Delta t} - \frac{L_1+L_2}{4c\Delta t}\right)\|\delta_t\phi^{n+1}\|_{H^{-1}}^2 - \left(A\Delta t - \frac{(L_1+L_2)c\Delta t}{4}\right)\|\nabla\delta_t\phi^{n+1}\|_{L^2}^2\end{aligned}$$

$$-\left(\frac{B}{2}-\frac{L_1+L_2}{4}\right)\|\delta_t\phi^{n+1}-\delta_t\phi^n\|_{L^2}^2,$$

where we have used $\|\delta_t\phi^{n+1}\|_{L^2}^2 = \|\delta_t\phi^{n+1}\|_{H^{-1}}\|\nabla\delta_t\phi^{n+1}\|_{L^2} \le \frac{1}{2c\Delta t}\|\delta_t\phi^{n+1}\|_{H^{-1}}^2 + \frac{c\Delta t}{2}\|\nabla\delta_t\phi^{n+1}\|_{L^2}^2$ for any $c > 0$ [19]. With $c = \frac{M(L_1+L_2)}{4\beta}$, $A \ge \frac{M(L_1+L_2)^2}{16\beta}$, and $B \ge \frac{L_1+L_2}{2}$, we have $\tilde{\mathcal{F}}^{n+1} - \tilde{\mathcal{F}}^n \le 0$. □

3. Numerical experiments

3.1. Numerical implementation

The scheme (2.1)-(2.2) can be expressed as follows:

$$\begin{aligned}
&\left(\frac{1}{\Delta t}-\frac{M\Delta t}{2\alpha+\beta\Delta t}\Delta\left(\frac{1}{2}(1+\Delta)^2-A\Delta t\Delta+B\right)\right)\phi^{n+1}\\
&=\frac{\phi^n}{\Delta t}+\frac{M\Delta t}{2\alpha+\beta\Delta t}\Delta\left(f_{dou}(\phi^{*,n+\frac{1}{2}})+f_{vac}(\phi^{*,n+\frac{1}{2}})+\frac{1}{2}(1+\Delta)^2\phi^n+A\Delta t\Delta\phi^n+B(-2\phi^n+\phi^{n-1})\right)\\
&\quad+\frac{2\alpha}{2\alpha+\beta\Delta t}\psi^n,\\
&\psi^{n+1}=2\frac{\phi^{n+1}-\phi^n}{\Delta t}-\psi^n.
\end{aligned}$$

For the first equation with the periodic boundary condition, we can use the Fourier spectral method [20–22] for achieving efficient computations.

For the energy stability, we replace $F_{dou}(\phi)$ and $F_{vac}(\phi)$, respectively, by

$$\tilde{F}_{dou}(\phi)=\begin{cases}\frac{3p^2-\epsilon}{2}\phi^2-2p^3\phi+\frac{3p^4}{4}, & \phi>p\\ \frac{1}{4}\phi^4-\frac{\epsilon}{2}\phi^2, & \phi\in[-p,p]\\ \frac{3p^2-\epsilon}{2}\phi^2+2p^3\phi+\frac{3p^4}{4}, & \phi<-p\end{cases}$$

and

$$\tilde{F}_{vac}(\phi)=\begin{cases}0, & \phi>0\\ -\frac{2h_{vac}}{3}\phi^3, & \phi\in[-q,0]\\ \frac{2h_{vac}}{3}(3q\phi^2+3q^2\phi+q^3), & \phi<-q,\end{cases}$$

where $p, q > 0$ are constants. It is then obvious that there exist L_1 and L_2 such that (2.5) is satisfied with f_i replaced by $\tilde{f}_i = \tilde{F}_i'$ for $i = dou$ and vac. Unless otherwise stated, we set $p = 1$, $r = 5$, $q = \frac{r}{h_{vac}}$, $L_1 = 3p^2 - \epsilon$, $L_2 = 4h_{vac}q = 4r$, $A = \frac{M(L_1+L_2)^2}{16\beta}$, and $B = \frac{L_1+L_2}{2}$. We note that the stabilization parameters A and B are independent of h_{vac}.

3.2. Numerical verification of the convergence of the scheme and Theorems 1 and 3

First, we verify the convergence of the scheme using

$$\begin{aligned}\phi(x,y,0) &= 0.02\cos^2\left(\frac{\pi(x+10)}{32}\right)\sin^2\left(\frac{\pi(y+3)}{32}\right) - 0.01\sin^2\left(\frac{\pi x}{8}\right)\sin^2\left(\frac{\pi(y-6)}{8}\right)\\ &\quad -0.02\cos\left(\frac{\pi(x-12)}{16}\right)\sin\left(\frac{\pi(y-1)}{16}\right) + 0.07, \quad \psi(x,y,0) = 0\end{aligned}$$

and take $\Omega = [0,32]^2$, $\Delta x = \Delta y = \frac{1}{3}$, $\alpha = 1$, $\beta = 1$, $M = 1$, and $\epsilon = 0.025$. Figure 1 shows the relative l_2-errors of $\phi(x,y,40)$ with $h_{vac} = 10$, 100, and 1000 for $\Delta t = 2^{-9}, 2^{-8}, \ldots, 1$, where the error is calculated compared to the reference solution using $\Delta t = 2^{-11}$. It is observed that the convergence order is 2 regardless of h_{vac} and the convergence constant is not affected by h_{vac}.

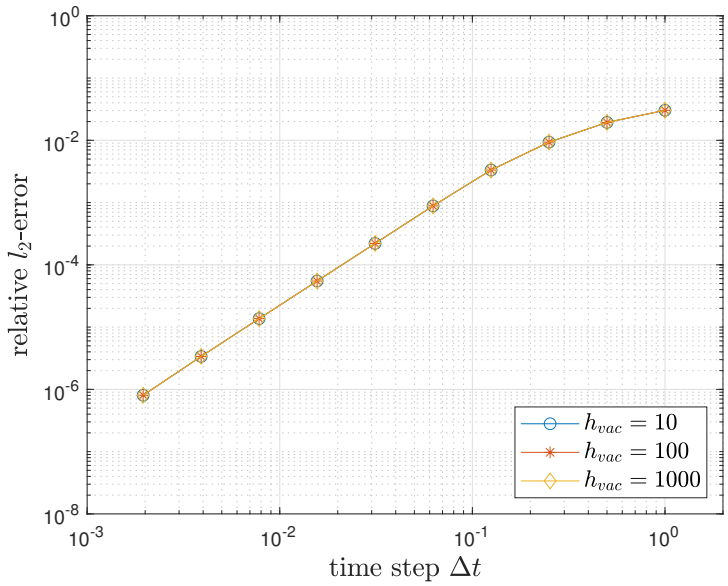

Figure 1. Errors of $\phi(x,y,40)$ with different h_{vac} for various Δt.

Next, we verify Theorems 1 and 3 using

$$\phi(x,y,0) = 0.06 + rand(x,y), \quad \psi(x,y,0) = 0$$

and set $\Omega = [0,128]^2$, $\Delta x = \Delta y = 1$, $\alpha = 0.01$, $\beta = 1$, $M = 1$, and $\epsilon = 0.9$, where $rand(x,y)$ is a random number between -0.01 and 0.01 at the grid points. Figure 2(a,b) show the evolution of $\int_\Omega \phi(x,y,t)\,dxdy$ and $\tilde{\mathcal{F}}(t)$, respectively, with $h_{vac} = 5000$ and 500000 for $\Delta t = 2^{-2}, 2^{-1}, \ldots, 2^6$. As proved by Theorems 1 and 3, the masses are conserved, and the energies decrease monotonically regardless of h_{vac}. Moreover, the energy decay trend is not affected by h_{vac}. Figure 3(a,b) show the evolution of $\phi(x,y,t)$ with $\Delta t = 2^{-2}$ for $h_{vac} = 5000$ and 500000, respectively.

And, to investigate the effect of A and B on the energy stability, we perform simulations with small A and B. Figure 4 shows the evolution of $\tilde{\mathcal{F}}(t)$ with small A and B for $h_{vac} = 5000$. In Figure 4(a,b), $A = \frac{1}{100}\frac{M(L_1+L_2)^2}{16\beta}$ and $B = \frac{1}{100}\frac{L_1+L_2}{2}$ lead to the increase of the energy because they do not satisfy the stability condition ($A \geq \frac{M(L_1+L_2)^2}{16\beta}$ and $B \geq \frac{L_1+L_2}{2}$, Theorem 3).

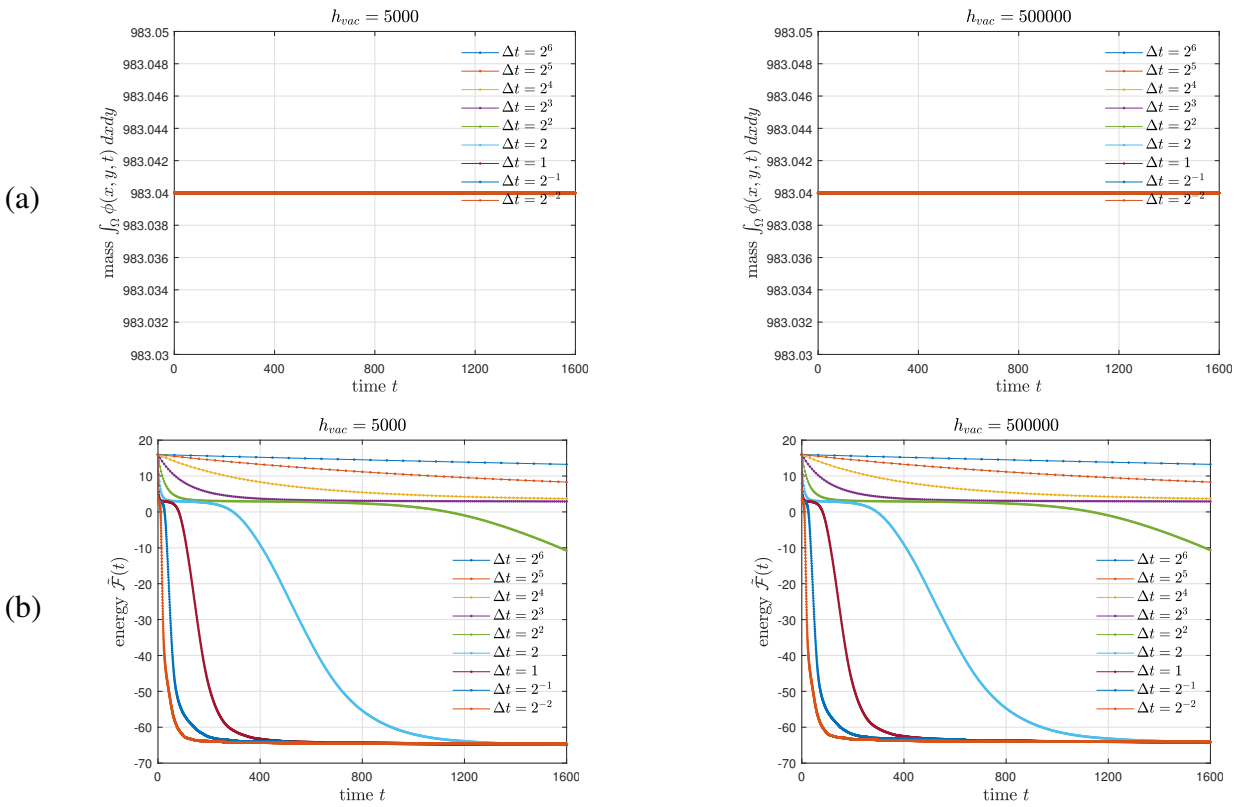

Figure 2. Evolution of (a) $\int_\Omega \phi(x,y,t)\,dxdy$ and (b) $\tilde{\mathcal{F}}(t)$ with different h_{vac} for various Δt.

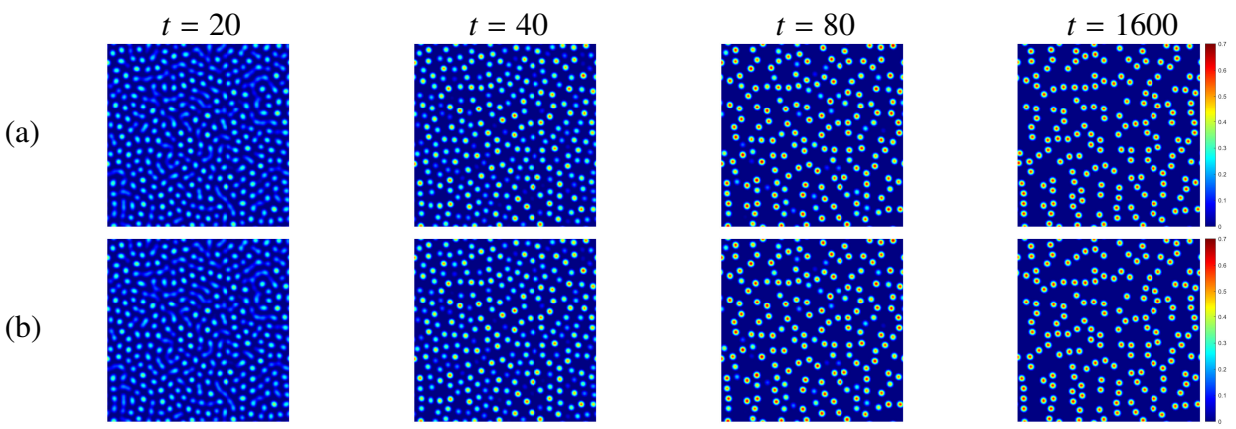

Figure 3. Evolution of $\phi(x,y,t)$ with $\bar{\phi} = 0.06$ for (a) $h_{vac} = 5000$ and (b) 500000.

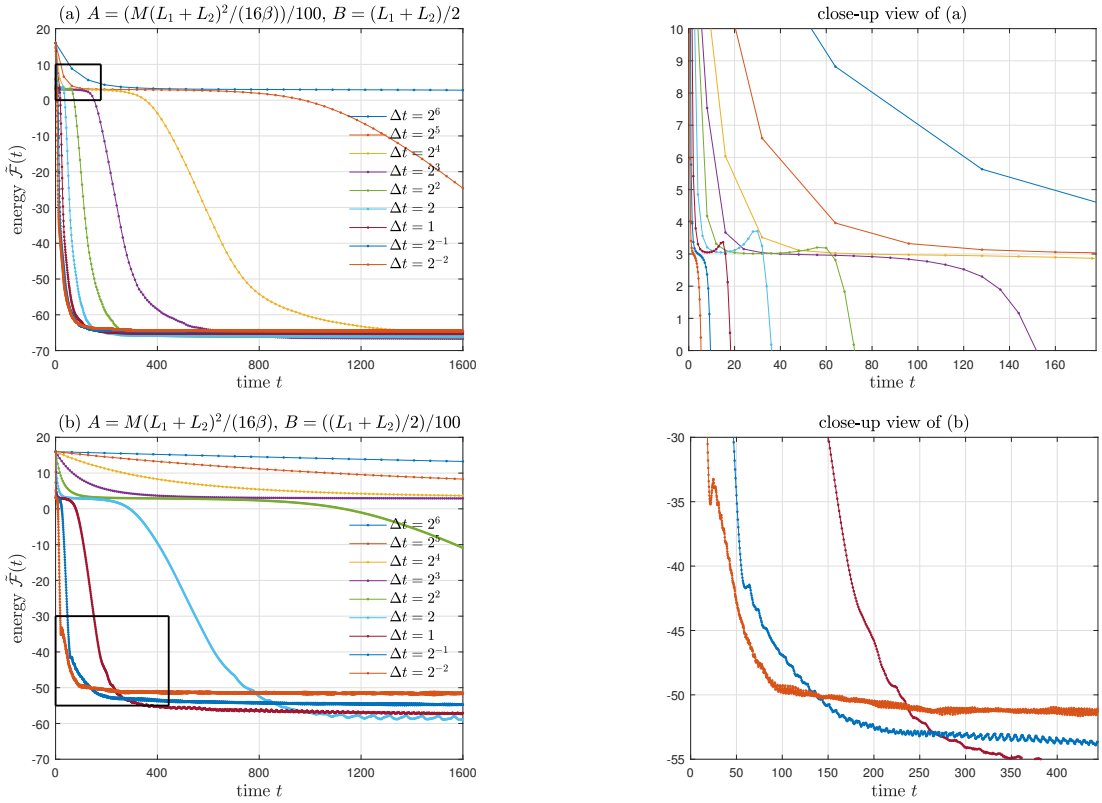

Figure 4. Evolution of $\tilde{\mathcal{F}}(t)$ with small A and B for various Δt, where $h_{vac} = 5000$.

3.3. Influence of the vacancy potential on the evolution

To explore the influence of the vacancy potential on the evolution, we employ

$$\phi(x, y, z, 0) = \bar{\phi} + rand(x, y, z), \quad \psi(x, y, z, 0) = 0$$

and take $\Omega = [0, 32]^3$, $\Delta x = \Delta y = \Delta z = \frac{1}{2}$, $\Delta t = \frac{1}{4}$, $\alpha = 1$, $\beta = 0.8$, $M = 1$, and $\epsilon = 0.9$, where $rand(x, y, z)$ is a random number between -0.01 and 0.01 at the grid points. Figures 5 and 6 show $\phi(x, y, z, 320)$ without the vacancy potential ($h_{vac} = 0$) and with the vacancy potential ($h_{vac} = 3000$), respectively, for $\bar{\phi} = 0.06$, 0.11, and 0.16. The evolution of $\tilde{\mathcal{F}}(t)$ is shown in Figure 7. For $h_{vac} = 0$, no vacancies appear even when $\bar{\phi} = 0.06$. In contrast, for $h_{vac} = 3000$, there are many vacancies. At the same time, the number of atoms increases with $\bar{\phi}$. The simulation results are in good agreement with those of [12].

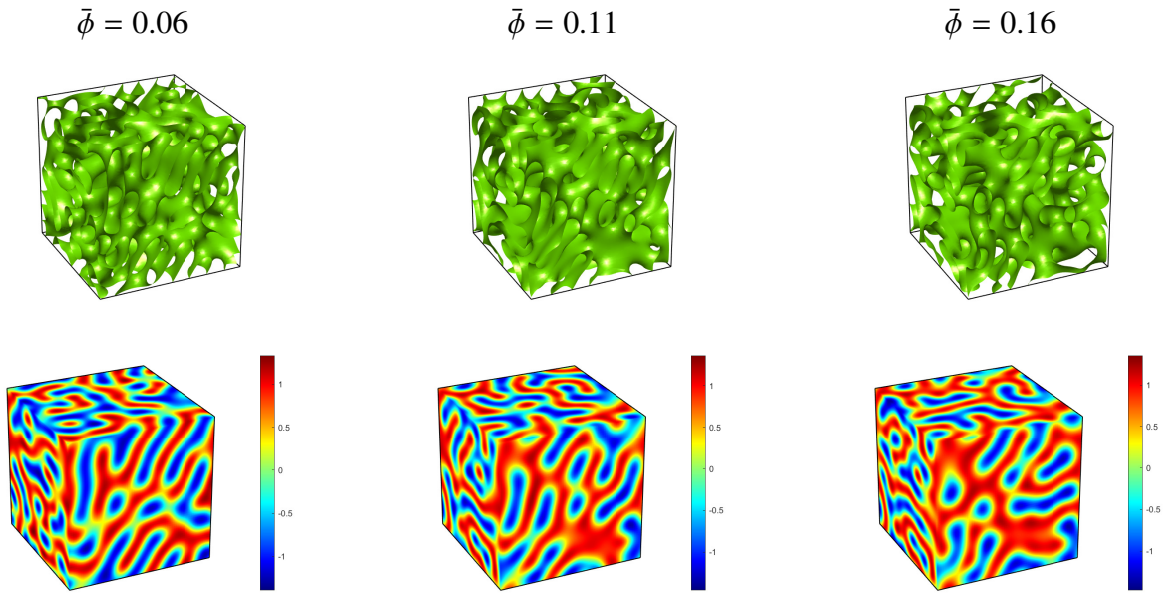

Figure 5. $\phi(x, y, z, 320)$ without the vacancy potential ($h_{vac} = 0$) for various $\bar{\phi}$ (from left to right). Top: an isosurface of $\phi = 0$; bottom: a slice of ϕ across the indicated plane.

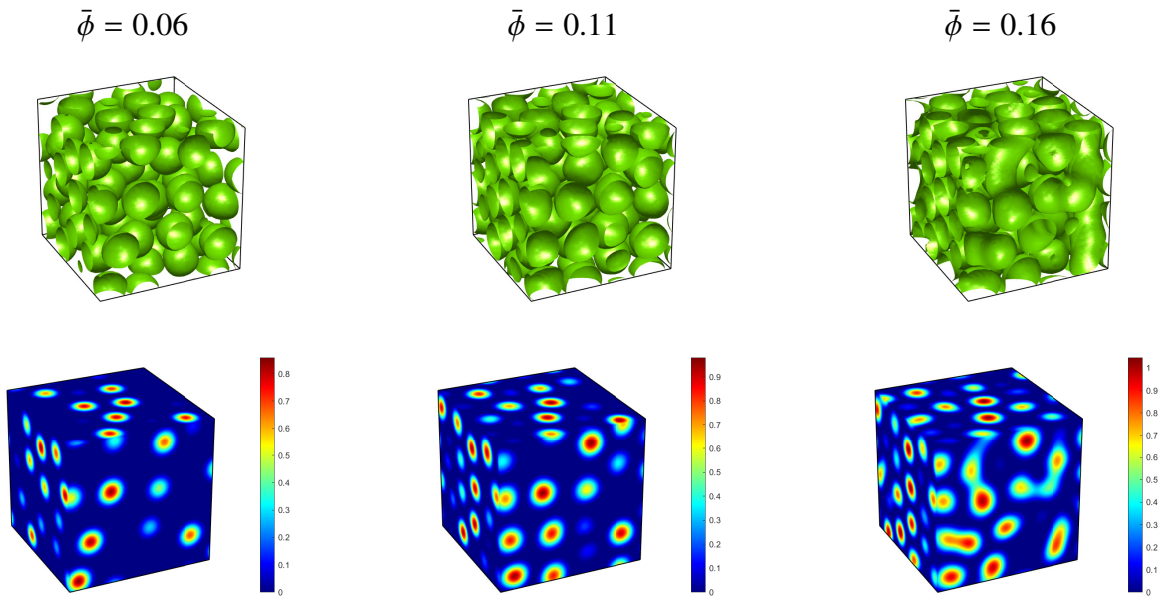

Figure 6. $\phi(x, y, z, 320)$ with the vacancy potential ($h_{vac} = 3000$) for various $\bar{\phi}$ (from left to right). Top: an isosurface of $\phi = 0$; bottom: a slice of ϕ across the indicated plane.

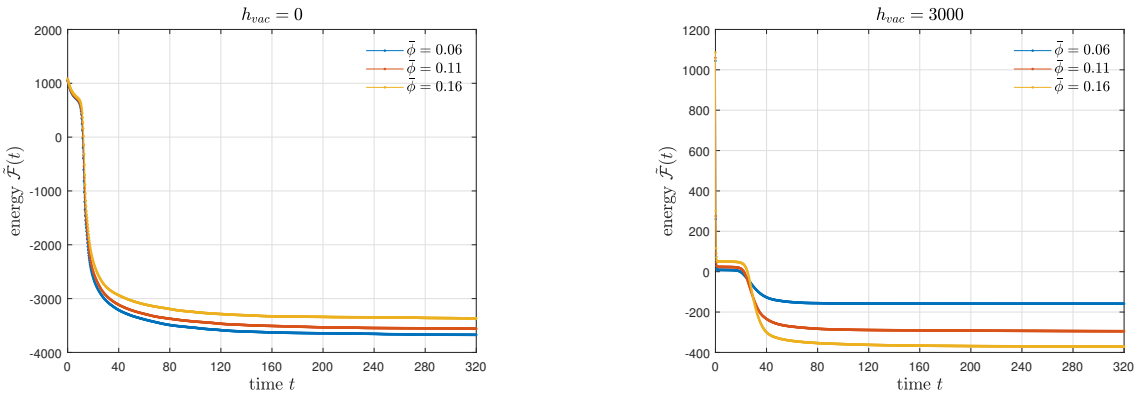

Figure 7. Evolution of $\tilde{\mathcal{F}}(t)$ with different h_{vac} for various $\bar{\phi}$.

4. Conclusions

We presented the efficient and energy-stable scheme based on the CN formula for the VMPFC equation. In the scheme, $f_{dou}(\phi)$ and $f_{vac}(\phi)$ were treated explicitly, which made the scheme efficient, and the energy stability was guaranteed by assuming that $\max_{\phi\in\mathbb{R}} |f'_{dou}(\phi)| \leq L_1 = 3p^3 - \epsilon$ and $\max_{\phi\in\mathbb{R}} |f'_{vac}(\phi)| \leq L_2 = 4r$ and by adding $-A\Delta t\Delta\delta_t\phi^{n+1}$ and $B(\delta_t\phi^{n+1} - \delta_t\phi^n)$. We proved that the scheme is energy-stable under $A \geq \frac{M(L_1+L_2)^2}{16\beta}$ and $B \geq \frac{L_1+L_2}{2}$ which are independent of h_{vac}. Through numerical experiments, it was observed that (i) our scheme is second-order accurate in time, mass-conservative, energy-stable, and suitable for simulating vacancies; and (ii) the convergence constant and energy decay trend are not affected by h_{vac}.

In future work, we have a plan to carry out a rigorous error analysis for the scheme and to analyze the stability of the scheme.

Use of Generative-AI tools declaration

The author declares they have not used Artificial Intelligence (AI) tools in the creation of this article.

Acknowledgments

The corresponding author (H.G. Lee) thanks the reviewers for the constructive and helpful comments on the revision of this article and was supported by the National Research Foundation of Korea (NRF) grant funded by the Korea government (MSIT) (No. RS-2022-NR069708).

Conflict of interest

The author declares no conflict of interest in this paper.

References

1. L. Q. Chen, Phase-field models for microstructure evolution, *Annu. Rev. Mater. Res.*, **32** (2002), 113–140. https://doi.org/10.1146/annurev.matsci.32.112001.132041

2. B. Xia, X. Xi, R. Yu, P. Zhang, Unconditional energy-stable method for the Swift–Hohenberg equation over arbitrarily curved surfaces with second-order accuracy, *Appl. Numer. Math.*, **198** (2024), 192–201. https://doi.org/10.1016/j.apnum.2024.01.005
3. X. Hu, Q. Xia, B. Xia, Y. Li, A second-order accurate numerical method with unconditional energy stability for the Lifshitz–Petrich equation on curved surfaces, *Appl. Math. Lett.*, **163** (2025), 109439. https://doi.org/10.1016/j.aml.2024.109439
4. W. Xie, Z. Wang, J. Kim, X. Sun, Y. Li, A novel ensemble Kalman filter based data assimilation method with an adaptive strategy for dendritic crystal growth, *J. Comput. Phys.*, **524** (2025), 113711. https://doi.org/10.1016/j.jcp.2024.113711
5. Q. Xia, J. Yang, J. Kim, Y. Li, On the phase field based model for the crystalline transition and nucleation within the Lagrange multiplier framework, *J. Comput. Phys.*, **513** (2024), 113158. https://doi.org/10.1016/j.jcp.2024.113158
6. P. Stefanovic, M. Haataja, N. Provatas, Phase-field crystals with elastic interactions, *Phys. Rev. Lett.*, **96** (2006), 225504. https://doi.org/10.1103/PhysRevLett.96.225504
7. P. Stefanovic, M. Haataja, N. Provatas, Phase field crystal study of deformation and plasticity in nanocrystalline materials, *Phys. Rev. E*, **80** (2009), 046107. https://doi.org/10.1103/PhysRevE.80.046107
8. A. Baskaran, Z. Hu, J. S. Lowengrub, C. Wang, S. M. Wise, P. Zhou, Energy stable and efficient finite-difference nonlinear multigrid schemes for the modified phase field crystal equation, *J. Comput. Phys.*, **250** (2013), 270–292. https://doi.org/10.1016/j.jcp.2013.04.024
9. H. G. Lee, J. Shin, J. Y. Lee, First- and second-order energy stable methods for the modified phase field crystal equation, *Comput. Methods Appl. Mech. Engrg.*, **321** (2017), 1–17. https://doi.org/10.1016/j.cma.2017.03.033
10. Q. Li, L. Mei, X. Yang, Y. Li, Efficient numerical schemes with unconditional energy stabilities for the modified phase field crystal equation, *Adv. Comput. Math.*, **45** (2019), 1551–1580. https://doi.org/10.1007/s10444-019-09678-w
11. X. Li, J. Shen, Efficient linear and unconditionally energy stable schemes for the modified phase field crystal equation, *Sci. China Math.*, **65** (2022), 2201–2218. https://doi.org/10.1007/s11425-020-1867-8
12. P. Y. Chan, N. Goldenfeld, J. Dantzig, Molecular dynamics on diffusive time scales from the phase-field-crystal equation, *Phys. Rev. E*, **79** (2009), 035701. https://doi.org/10.1103/PhysRevE.79.035701
13. J. Zhang, X. Yang, Efficient second order unconditionally stable time marching numerical scheme for a modified phase-field crystal model with a strong nonlinear vacancy potential, *Comput. Phys. Commun.*, **245** (2019), 106860. https://doi.org/10.1016/j.cpc.2019.106860
14. Q. Li, X. Yang, L. Mei, Efficient numerical scheme for the anisotropic modified phase-field crystal model with a strong nonlinear vacancy potential, *Commun. Math. Sci.*, **19** (2021), 355–381. https://dx.doi.org/10.4310/CMS.2021.v19.n2.a3

15. N. Cui, P. Wang, Q. Li, A second-order BDF scheme for the Swift–Hohenberg gradient flows with quadratic–cubic nonlinearity and vacancy potential, *Comp. Appl. Math.*, **41** (2022), 85. https://doi.org/10.1007/s40314-022-01801-w

16. S. Pei, Y. Hou, W. Yan, Efficient unconditionally stable numerical schemes for a modified phase field crystal model with a strong nonlinear vacancy potential, *Numer. Meth. Part Differ. Equ.*, **38** (2022), 65–101. https://doi.org/10.1002/num.22828

17. X. Zhang, J. Wu, Z. Tan, Highly efficient, decoupled and unconditionally stable numerical schemes for a modified phase-field crystal model with a strong nonlinear vacancy potential, *Comput. Math. Appl.*, **132** (2023), 119–134. https://doi.org/10.1016/j.camwa.2022.12.011

18. H. G. Lee, A linear second-order convex splitting scheme for the modified phase-field crystal equation with a strong nonlinear vacancy potential, *Appl. Math. Lett.*, **156** (2024), 109145. https://doi.org/10.1016/j.aml.2024.109145

19. Q. Li, L. Mei, B. You, A second-order, uniquely solvable, energy stable BDF numerical scheme for the phase field crystal model, *Appl. Numer. Math.*, **134** (2018), 46–65. https://doi.org/10.1016/j.apnum.2018.07.003

20. D. D. Dai, W. Zhang, Y. L. Wang, Numerical simulation of the space fractional $(3+1)$-dimensional Gray–Scott models with the Riesz fractional derivative, *AIMS Math.*, **7** (2022), 10234–10244. https://doi.org/10.3934/math.2022569

21. X. Y. Li, Y. L. Wang, Z. Y. Li, Numerical simulation for the fractional-in-space Ginzburg–Landau equation using Fourier spectral method, *AIMS Math.*, **8** (2023), 2407–2418. https://doi.org/10.3934/math.2023124

22. S. F. Alrzqi, F. A. Alrawajeh, H. N. Hassan, An efficient numerical technique for investigating the generalized Rosenau–KDV–RLW equation by using the Fourier spectral method, *AIMS Math.*, **9** (2024), 8661–8688. https://doi.org/10.3934/math.2024420

Appendix

The MATLAB code for the numerical scheme in 2D (Figure 3(a)) is given as follows.

```
alpha=0.01; beta=1; M=1; epsilon=0.9; hvac=5000;
p=1; r=5; q=r/hvac; L1=3*p^2-epsilon; L2=4*r; A=M*(L1+L2)^2/(16*beta); B=(L1+L2)/2;

x1=0; xr=128; y1=0; yr=128; T=1600;
nx=128; ny=128; dx=(xr-x1)/nx; dy=(yr-y1)/ny; dt=2^-2; nt=round(T/dt);

x=x1:dx:xr-dx; y=y1:dy:yr-dy; [X,Y]=ndgrid(x,y);
xix=1i*2*pi*fftshift(-nx/2:nx/2-1)/(xr-x1);
xiy=1i*2*pi*fftshift(-ny/2:ny/2-1)/(yr-y1); [xiX,xiY]=ndgrid(xix,xiy);

ophi=0.06+0.01*(2*rand(nx,ny)-1); oophi=ophi; opsi=zeros(nx,ny);
xi_lap=xiX.^2+xiY.^2; L=1/dt-M*dt/(2*alpha+beta*dt)*xi_lap.*(1/2*(1+xi_lap).^2-A*dt*xi_lap+B);

for it=1:nt
hat=(3*ophi-oophi)/2;
rhs=ophi/dt+M*dt/(2*alpha+beta*dt)*Lap(fdou(hat,epsilon,p)+fvac(hat,hvac,q)+1/2*Lap2(ophi,xi_lap)+...
A*dt*Lap(ophi,xi_lap)+B*(-2*ophi+oophi),xi_lap)+2*alpha/(2*alpha+beta*dt)*opsi;
nphi=real(ifft2(fft2(rhs)./L)); npsi=2*(nphi-ophi)/dt-opsi;
oophi=ophi; ophi=nphi; opsi=npsi;
end

function val=fdou(phi,epsilon,p)
ind1=phi>p; ind2=phi<-p;
val=((3*p^2-epsilon)*phi-2*p^3).*ind1+(phi.^3-epsilon*phi).*(1-ind1).*(1-ind2)+...
((3*p^2-epsilon)*phi+2*p^3).*ind2;
end

function val=fvac(phi,hvac,q)
ind1=phi>0; ind2=phi<-q;
val=0.*ind1+(-2*hvac*phi.^2).*(1-ind1).*(1-ind2)+(2*hvac/3*(6*q*phi+3*q^2)).*ind2;
end

function val=Lap(phi,xi_lap)
val=real(ifft2(fft2(phi).*xi_lap));
end

function val=Lap2(phi,xi_lap)
val=real(ifft2(fft2(phi).*(1+xi_lap).^2));
end
```

The MATLAB code for the numerical scheme in 3D (Figure 6) is given as follows.

```
alpha=1; beta=0.8; M=1; epsilon=0.9; hvac=3000;
p=1; r=5; q=r/hvac; L1=3*p^2-epsilon; L2=4*r; A=M*(L1+L2)^2/(16*beta); B=(L1+L2)/2;

x1=0; xr=32; y1=0; yr=32; z1=0; zr=32; T=320;
nx=64; ny=64; nz=64; dx=(xr-x1)/nx; dy=(yr-y1)/ny; dz=(zr-z1)/nz; dt=2^-2; nt=round(T/dt);

x=x1:dx:xr-dx; y=y1:dy:yr-dy; z=z1:dz:zr-dz; [X,Y,Z]=ndgrid(x,y,z);
xix=1i*2*pi*fftshift(-nx/2:nx/2-1)/(xr-x1);
xiy=1i*2*pi*fftshift(-ny/2:ny/2-1)/(yr-y1);
xiz=1i*2*pi*fftshift(-nz/2:nz/2-1)/(zr-z1); [xiX,xiY,xiZ]=ndgrid(xix,xiy,xiz);

ophi=0.06+0.01*(2*rand(nx,ny,nz)-1); oophi=ophi; opsi=zeros(nx,ny,nz);
xi_lap=xiX.^2+xiY.^2+xiZ.^2; L=1/dt-M*dt/(2*alpha+beta*dt)*xi_lap.*(1/2*(1+xi_lap).^2-A*dt*xi_lap+B);

for it=1:nt
hat=(3*ophi-oophi)/2;
rhs=ophi/dt+M*dt/(2*alpha+beta*dt)*Lap(fdou(hat,epsilon,p)+fvac(hat,hvac,q)+1/2*Lap2(ophi,xi_lap)+...
A*dt*Lap(ophi,xi_lap)+B*(-2*ophi+oophi),xi_lap)+2*alpha/(2*alpha+beta*dt)*opsi;
nphi=real(ifftn(fftn(rhs)./L)); npsi=2*(nphi-ophi)/dt-opsi;
oophi=ophi; ophi=nphi; opsi=npsi;
end

function val=fdou(phi,epsilon,p)
ind1=phi>p; ind2=phi<-p;
val=((3*p^2-epsilon)*phi-2*p^3).*ind1+(phi.^3-epsilon*phi).*(1-ind1).*(1-ind2)+...
((3*p^2-epsilon)*phi+2*p^3).*ind2;
end

function val=fvac(phi,hvac,q)
ind1=phi>0; ind2=phi<-q;
val=0.*ind1+(-2*hvac*phi.^2).*(1-ind1).*(1-ind2)+(2*hvac/3*(6*q*phi+3*q^2)).*ind2;
end

function val=Lap(phi,xi_lap)
val=real(ifftn(fftn(phi).*xi_lap));
end

function val=Lap2(phi,xi_lap)
val=real(ifftn(fftn(phi).*(1+xi_lap).^2));
end
```

AIMS Press

© 2025 the Author(s), licensee AIMS Press. This is an open access article distributed under the terms of the Creative Commons Attribution License (https://creativecommons.org/licenses/by/4.0)